Primljen / Received: 27.12.2024.
Ispravljen / Corrected: 27.4.2025.
Prihvaćen / Accepted: 25.6.2025..
Dostupno online / Available online: 10.8.2025.

Deformation control for a five-story deep excavation

Authors:

[1]Ping Chen, MSc. CE
chenping@ziad.cn
Corresponding author

[1]Xingwang Liu, PhD. CE
liuxingwang@ziad.cn

[1]Guoqiang Cao, MSc. CE
caoguoqiang@ziad.cn

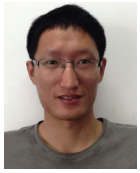

[1]Yongxing He, PhD. CE
heyongxing@ziad.cn

[2]Anming Xu, MSc. CE
22312247@zju.edu.cn

[1] Zhejiang Institute of Architectural Design and Research Co. Ltd, Zhejiang, China
[2] Zhejiang University, China
College of Civil Engineering and Architecture

Professional paper

Ping Chen, Xingwang Liu, Guoqiang Cao, Yongxing He, Anming Xu

Deformation control for a five-story deep excavation

The Hangzhou Hang Lung Plaza features a five-story basement close to a cluster of old, shallow-founded buildings along its 365 m eastern side that are extremely sensitive to deformation. To address the challenges of deformation control, this project employed not only traditional rigid retaining structures of diaphragm walls combined with internal struts but also active protection technologies, such as zoned excavation, cross walls, and axial force servo-controlled concrete struts. The monitoring results indicated that the aforementioned technologies markedly reduced the horizontal deformation of the retaining walls, with a maximum reduction of approximately 43 %, thereby ensuring control of the excavation deformation and facilitating the safety of adjacent buildings. This study validated the effectiveness of zoned excavation, cross walls, and servo-controlled struts under soft soil conditions; however, further research is required to optimize specific parameters and integrate dynamic adjustment algorithms for broader adaptability.

Key words:
deep excavation, deformation control, shallow foundation buildings, zoned excavation, cross walls, axial force servo-controlled struts

Stručni rad

Ping Chen, Xingwang Liu, Guoqiang Cao, Yongxing He, Anming Xu

Kontrola deformacija pri iskopu dubine pet etaža

Zgrada Hang Lung Plaza u Hangzhouu obuhvaća pet etaža podzemnog prostora, smještenog uz istočnu granicu gradilišta, dugu 365 m, u neposrednoj blizini skupine starijih zgrada s plitkim temeljima koje su vrlo osjetljive na deformacije. Radi učinkovite kontrole deformacija, u tom su projektu uz uobičajenu krutu potporu izvedenu pomoću membranskih zidova i unutarnjih podupirača primijenjene i aktivne zaštitne tehnologije: fazni iskop, poprečni zidovi te servoupravljani betonski podupirači s kontrolom aksijalne sile. Rezultati praćenja pokazali su da su navedene tehnologije znatno smanjile horizontalne deformacije potpornih zidova, s maksimalnim smanjenjem od približno 43 %, čime je omogućena kontrola deformacija iskopa i osigurana sigurnost susjednih građevina. Istraživanje potvrđuje učinkovitost faznog iskopa, poprečnih zidova i servoupravljanih podupirača u uvjetima mekih tala. Ipak, za njihovu širu primjenu potrebna su dodatna istraživanja radi optimiranja pojedinih parametara te integracije algoritama za dinamičko prilagođavanje.

Ključne riječi:
duboki iskop, kontrola deformacija, građevine s plitkim temeljima, fazni iskop, poprečni zidovi, servoupravljani podupirači s kontrolom aksijalne sile

1. Introduction

As China vigorously promotes the development of underground spaces, the scale of excavation, specifically ultra-deep and ultra-large excavations, is increasing. Against the backdrop of organically renewing cities, the environment surrounding excavation work is becoming increasingly complex. Excavations are now commonly undertaken adjacent to sensitive protected objects such as rail transit facilities, shallow-founded old buildings, and cultural heritage buildings. For deep and large excavations under complex conditions, in addition to guaranteeing their safety and stability, ensuring reasonable and effective deformation control to avoid adverse effects on the environment and the normal use of surrounding buildings and structures is crucial and worthy of research.

Because of the rheological properties of soft soils, deformation control has always been an important topic in the study of deep excavations in areas with these soils. Although traditional methods, such as anchored walls and hybrid support systems, are widely used and effective in general excavation projects, deep and large-scale excavations in soft soil with adjacent sensitive structures often require more robust solutions, including diaphragm walls combined with multiple internal concrete struts and even large-scale pre-construction soil improvement to ensure deformation control within acceptable limits [1-5]. Liu et al., based on the engineering practice of the Hangzhou Center project with a six-story deep excavation, proposed a series of subway facility protection technologies, including quantitative control for the spatiotemporal effect of deep and large excavations in soft soil, active reinforcement technology for the side and bottom of existing tunnels, and three-dimensional numerical simulation technology based on the hypoplastic model for structured soft clay [6]. Technologies such as zoned excavation, isolation piles, and axial-force servo-controlled steel struts have been successfully applied in deep excavations adjacent to subway facilities [7-11]. The mechanism of the cross-wall is similar to that of a strut component, with a high compressive strength already present before excavation. After excavation, the deformation of the retaining wall at the position of the cross wall is restrained, and the lateral displacement of the retaining wall can be significantly reduced, thereby reducing ground settlement outside the excavation area and ensuring environmental protection [12-15]. Recent research on deep excavations in complex geotechnical conditions has underscored the importance of adaptive support systems [16]. This concept is inherently aligned with the design philosophy of servo-controlled axial force struts, which not only eliminates strut deformation through prestressing but also reduces deformation of the retaining structure and adjacent protected objects, as demonstrated in their successful application to a deep excavation in Hongkou District, Shanghai, ensuring the uninterrupted operation of a neighboring subway tunnel [17-21]. A reasonable excavation sequence and informatized construction are crucial for deformation control in deep and large excavation [22-24]. Notably, many similar studies have been conducted on the deformation control of deep excavations based on actual projects. Environmental protection objects are often subway facilities, which may be related to the rapid development of rail-transit construction in recent years. However, there have been few studies on the protection of shallow-founded buildings, even though they are also sensitive environmental objects.

In this study, the deep excavation of Hangzhou Hang Lung Plaza, which has a five-story basement, was used as the research object to investigate protection technologies such as zoned excavation, cross walls, and axial force servo-controlled concrete struts for old residential buildings with shallow foundations. In addition, the effectiveness of these technologies was analyzed through field measurements. The findings provide a reference for deep and large excavations in soft soil areas under similar environmental conditions.

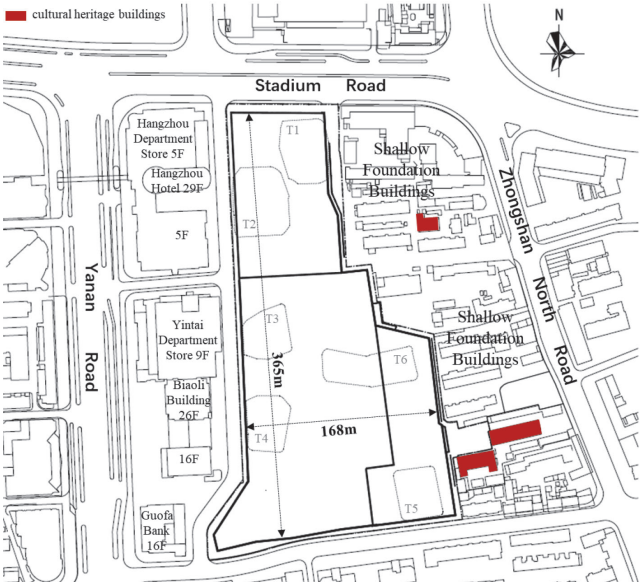

Figure 1. General excavation plan

2. Project overview

Hangzhou's Hang Lung Plaza is located in a prime downtown area at the intersection of Stadium Road and Zhongshan North Road and covers a total land area of approximately 52,100 m^2. The aboveground structure consists of one super high-rise office building, five high-rise office buildings, and their podiums, as well as a five-story basement. The excavation plan is roughly rectangular, with dimensions of approximately 365 × 168 m, and the general excavation depth ranges from 28.4 to 29.7 m, with the core tube dropping to a depth of 4.6 to 6.4 m.

The surrounding environmental conditions of the project are complex and have high protection requirements. To the north of the excavation is Stadium Road, an important urban artery with a large traffic flow. To the west is the Dazhi Lane, with landmark buildings such as the Intime Department Store and the Biaoli Building across the road. To the south is the Bai Jing Fang Lane, which is opposite the residential land tract. To the east, it is adjacent to a 365 m long cluster of old buildings with shallow foundations along the north–

Table 1. Physical and mechanical parameters of the soil layers

Soil layer	Thickness [m]	Unit weight [kN/m³]	Consolidated quick shear test	
			Cohesion [kPa]	Angle of friction [°]
1-0 miscellaneous fill	6.8 ~ 0.6	—	*3	*7
1-1 plain fill	4.7 ~ 0.6	16.80	*9	*6
1-2 silty clay	4.8 ~ 0.7	18.52	27.5	16.4
1-3 clayey silt	4.6 ~ 0.4	18.68	12.5	23.3
2-1 muddy clay	12.1 ~ 1.2	17.12	13.8	9.4
2-2 silty clay interlaid with silt	10.9 ~ 0.7	18.26	17.6	17.7
3-1 muddy-silty clay	10.7 ~ 0.1	17.26	15.0	10.0
3-2 silty clay	12.2 ~ 0.7	18.11	25.7	15.5
4 clay	15.3 ~ 1.8	18.48	46.7	21.0
6 silty clay	15.0 ~ 0.9	19.06	46.8	21.5
7-1 silty clay	10.5 ~ 1.2	18.84	40.1	20.4
7-2 silty fine sand	5.5 ~ 0.6	19.34	6.2	30.6
7-3 round gravel	2.4 ~ 0.8	—	—	—

south line, all of which are early constructed shallow-foundation houses. The closest distance to the retaining wall is only 5.5 m. Among the old buildings, two are cultural heritage buildings dating back to the 17th century. They have undergone multiple repairs and have complex and fragile internal structures. Therefore, the cluster of shallow-foundation buildings on the east side of the excavation, which is extremely sensitive to deformation, is the key environmental protection object of this project. In addition, numerous pipelines are present under the municipal roads surrounding the project, many of which are old and require repair. They also need to be strictly protected during excavation.

The topography of the site is characterized by a quaternary lake and a marsh sedimentary plain, and its soil layer distribution and physical and mechanical parameters are listed in Table 1. The surface fill in the excavation area is relatively thick: Layer 2-1 is silty clay, Layer 2-2 is silty clay interlaid with silt, and Layer 3-1 is muddy–silty clay, all of which are characterized by high compressibility, low strength, and high sensitivity. Below the pit bottom, Layer 7-2 silty fine sand and Layer 7-3 round gravel are aquifers, with the water head buried approximately 6 m below the ground surface and mainly distributed in the northern part of the site. The retaining wall penetrates and isolates the aquifer. The bedrock types in the deep part of the site are diverse and undulating, with tuff in the north and muddy siltstone in the south (with local conglomerate lenses). These bedrocks have a significant influence on the construction of the embedded diaphragm walls and foundation piles.

3. Active protection technologies for shallow foundation building

The excavation support system utilized a combination of diaphragm walls and multiple horizontal concrete struts. The overall rigidity of the support structure on the east side, which is adjacent to the shallow foundation building clusters, was further strengthened: a 1200 mm thick diaphragm wall was used in conjunction with trench cutting re-mixing deep wall (TRD) slot wall reinforcement, isolation piles with a diameter of 800 mm were added outside the pit, six horizontal struts were set up inside the pit, and a continuous passive zone reinforcement of cement soil mixing piles was set up inside the pit from the bottom of the third strut to the pit bottom, with a width of 8.7 m.

3.1. Zoned excavation

To protect the sensitive buildings on the east side, the large excavation was divided into smaller ones to control the scale of the pit adjacent to nearby buildings. Furthermore, the spatiotemporal effect was leveraged to mitigate the impact of excavation on the environment. The division of the pit should be combined with the floor plan of the main building and the functional zoning of the basement to minimize the division of the main building and ensure the integrity of the related functional areas. In addition, the division of the pit must consider the project development rhythm, and the estimated schedule should be within the target construction period. Based on the above considerations and the excavation outline, two internal partition walls were set up to subdivide the large excavation, which has a total area of approximately 44,650 m^2, into three areas: A, B, and C. Areas B and C, which are close to the shallow-foundation buildings, were 11,000 m^2 and 7,900 m^2, respectively. The east side, which was 365 m long, was further divided into three sections of 136, 48, and 168 m for separate excavations. The design process involved first excavating Zone A. After the basement of Zone A was completed, Zones B and C were simultaneously excavated. A detailed plan of each zone is shown in Figure 2. Because there were no soil removal conditions on the east and west sides of the site, three openings were set up in the

north–south direction. Zone A had a large amount of soil, and all three openings could be fully utilized during excavation to ensure efficient soil removal. Zones B and C could use openings 2 and 3, respectively, during the excavation stage without disturbing each other, thus achieving the design strategy of the zoned excavation. Owing to the suspension of work for the Hangzhou Asian Games, Zones B and C were excavated simultaneously after the completion of the foundation slab in Zone A to accelerate progress by strengthening strut force transmission and replacement measures. The ground reinforcement in the pit was strengthened to improve the efficiency of soil excavation, and the overall schedule target was ultimately achieved.

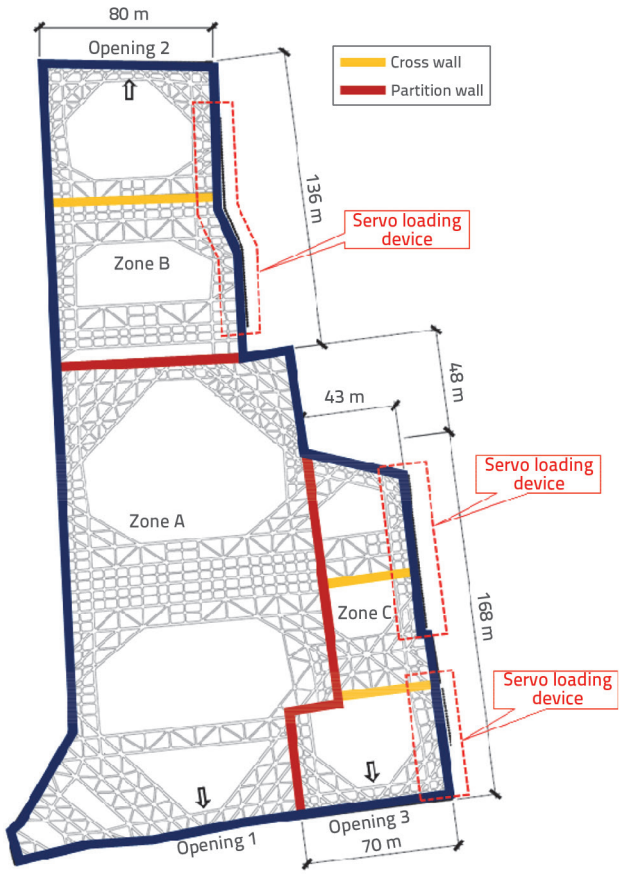

Figure 2. Layout plan for excavation zoning

3.2. Cross wall

After the division, the extensions of Zones B and C along the side close to the shallow-foundation buildings still reached 136 and 168 m, respectively. In particular, Zone C was adjacent to an important cultural heritage building, the Catholic Church, with the closest distance being only 8 m. Considering the layout of the buildings on the east side, the actual protection requirements, and the residents' concerns, a cross wall was set up in Zone B, and two cross walls were set up in Zone C, arranged perpendicular to the retaining wall. The support points were located at central positions where the spatiotemporal effect was poor. The aim was to form a rigid hidden support inside the pit to control the development of the lateral displacement of the retaining wall, thereby reducing the adverse effects of excavation on adjacent buildings. The cross walls were constructed using the same method as that used for the construction of the diaphragm wall, with a thickness of 1000 mm. The ground surface to the fifth strut was a plain concrete section, and the section from the fifth support to 10 m below the bottom of the pit was reinforced.

To further investigate the constraining effect of cross-wall planar layouts on retaining wall deformation, a three-dimensional finite element model of Zone C was developed based on actual engineering conditions and calibrated using field measurement data. Subsequently, computational models with varying cross-wall layouts were established based on the original model to analyze the deformation characteristics of the retaining wall under different in-pit cross-wall arrangements.

3.2.1. Establishment and validation of the original model

The diaphragm wall in Zone C had a depth of 49 m. The model selected a height of 60 m, with computational dimensions of 300 m (X-direction) × 400 m (Y-direction) × 60 m (Z-direction). For computational simplicity, the soil in the model was divided evenly into 10 layers. The soil was modeled using the Hardening Soil Small-strain (HSS) model, with the key parameters listed in Table 2. The structural materials were simplified based on equivalent stiffness principles: the retaining wall was modeled as a plate element of a specific thickness, and partial struts were modeled as beam elements using elastic constitutive models (parameters in Table 3). The boundary conditions followed the standard constraints:

Table 2. Soil distribution and model parameters

Soil layer	e_o	E_{50}^{ref} [kPa]	E_{oed}^{ref} [kPa]	E_{ur}^{ref} [kPa]	G_0^{ref} [kPa]	$\gamma_{0.7}$
1-0 miscellaneous fill	0.500	7.0	7.0	34.8	121	$2 \cdot 10^{-4}$
1-2 silty clay	0.893	7.0	4.9	32.0	120	$2 \cdot 10^{-4}$
2-1 muddy clay	1.294	3.4	2.3	15.9	33.3	$2 \cdot 10^{-4}$
2-2 silty clay interlaid with silt	0.924	3.9	3.0	24.0	48	$2 \cdot 10^{-4}$
3-1 muddy-silty clay	1.202	3.2	2.4	19.2	31.9	$2 \cdot 10^{-4}$
3-2 silty clay	0.987	5.2	4.0	32.0	64	$2 \cdot 10^{-4}$
4 clay	0.910	6.9	5.3	42.4	72.08	$2 \cdot 10^{-4}$
6 silty clay	0.776	7.5	5.8	46.4	92.8	$2 \cdot 10^{-4}$
Strongly weathered siltstone	0.678	30.0	30.0	180.0	600.0	$2 \cdot 10^{-4}$
Moderately weathered siltstone	0.500	50.0	50.0	300.0	800.0	$2 \cdot 10^{-4}$

horizontal constraints (UX=0, UY=0) on the lateral surfaces and vertical constraints (UZ=0) at the base. Groundwater effects were excluded by lowering the water table below the bottom of the excavation. To ensure the mesh quality, the soil was discretized using 15-node triangular plane-strain elements.

Table 3. Structural material calculation parameters

Components	*E* (×10⁴ MPa)	*EA* (×10⁷ kN/m)	*EI* (kN*m²/m)	ν
retaining wall	3.00	2.5	1.6×10⁶	0.2
concrete struts	3.00	3.00	—	0.2
structural slabs	3.00	2.70	1.82×10⁶	0.2

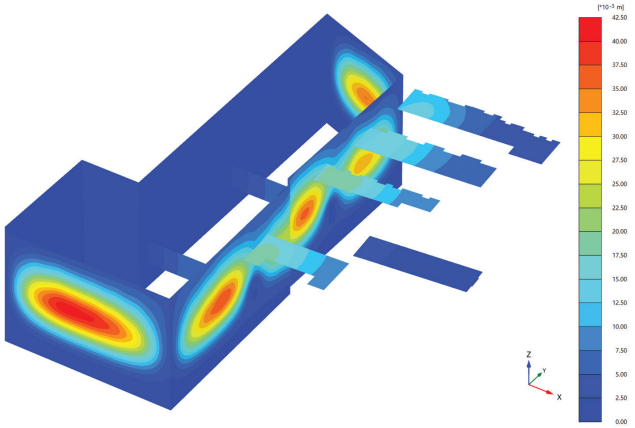

Figure 3. Total deformation contour map of Zone C

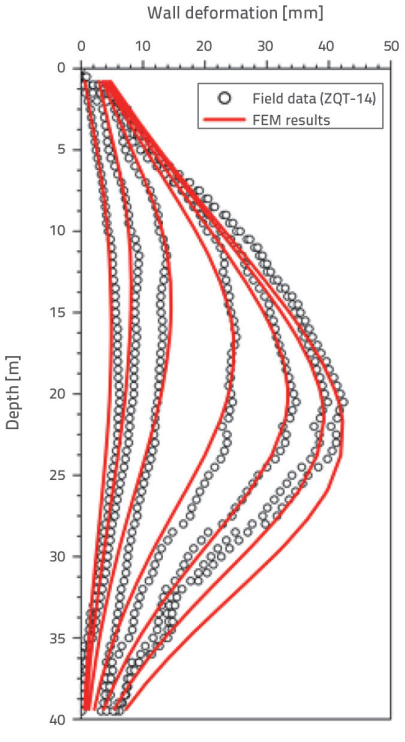

Figure 4. Computed wall deformation at ZQT-14 and comparison with the field measurements

The deformation contour map of the retaining wall after excavation of the bottom of the pit is shown in Figure 3. A comparison between the calculated and measured lateral displacements at the monitoring point ZQT-14 (east side) is shown in Figure 4. The model results aligned closely with field measurements, with minor discrepancies in deeper regions, likely owing to the assumption of uniform soil layers and isotropic properties in the model, which cannot fully reflect actual stratigraphic undulations or anisotropy. Overall, the model effectively captured the deformation behavior of the retaining wall during excavation.

3.2.2. Computational cases for different cross wall layouts

Zone C excavation was simplified into a 40 × 200 m rectangle for modeling. Adjacent structures, such as east-side buildings, temporary cultural relics stored to the north, and roads to the south, were converted into equivalent surcharge loads. The mesh layout is shown in Figure 5. Following the modeling approach described in Section 3.2.1, five scenarios were analyzed: 0, 1, 2, 3, and 4 cross walls (Figure 6).

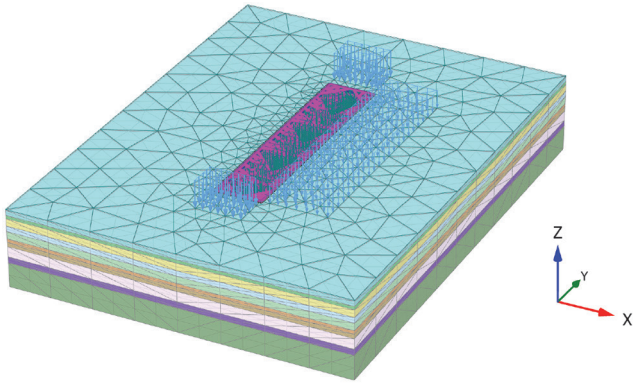

Figure 5. Overall mesh division

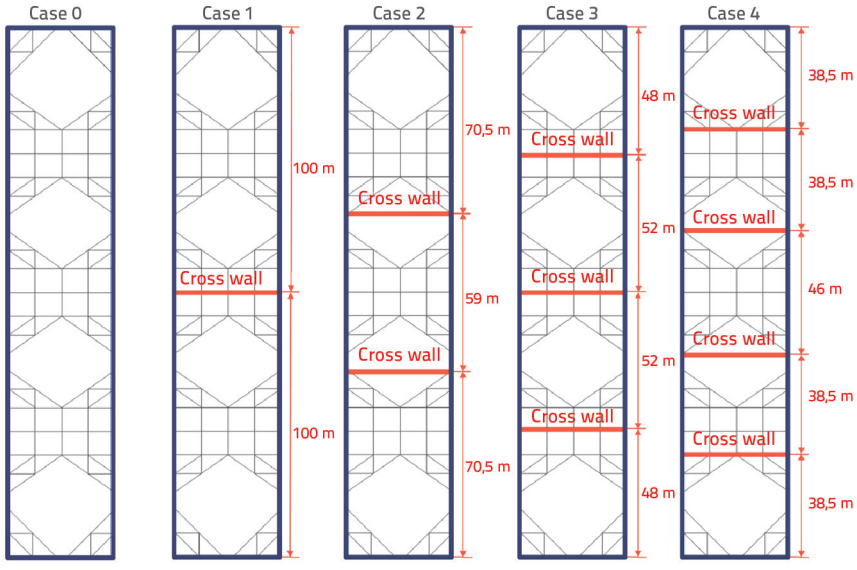

Figure 6. Planar layout of cross walls for different computational cases

3.2.3. Results and analysis

Compared to Case 0, installing one, two, three, and four cross walls reduced the eastern retaining wall deformation by 6.1%, 19.3%, 15.0%, and 30.0%, respectively. Notably, Case 2 achieved a significant deformation reduction. However, Case 3 showed slight deformation increases owing to the overlapping support struts and cross walls, which hindered their synergistic restraint. Case 4 further reduced deformation, but incremental gains diminished; adding two cross walls from Case 0 to Case 2 reduced deformation by 19.4%, whereas adding two more in Case 4 yielded only a 10.2% additional reduction.

The maximum deformation statistics at the retaining wall corners (cross-wall locations) and midspans (midpoints between two cross-walls on the retaining wall) for each case are illustrated in Figure 7, and the east retaining wall deformation distribution diagram is shown in Figure 8. It is evident that the deformation distribution of the retaining wall exhibited significantly non-uniform characteristics. In Case 1, the maximum displacement at the wall corner was only 14.67 mm, representing a 68.1% reduction, compared to the maximum mid-span displacement of 45.94 mm, which demonstrates the pronounced restraining effect of cross walls on localized deformation.

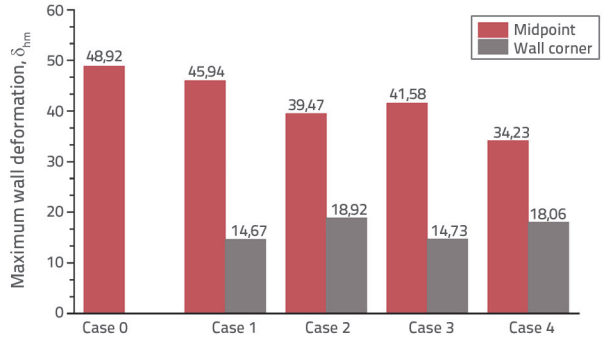

Figure 7. Maximum deformation at retaining wall corners and midspan

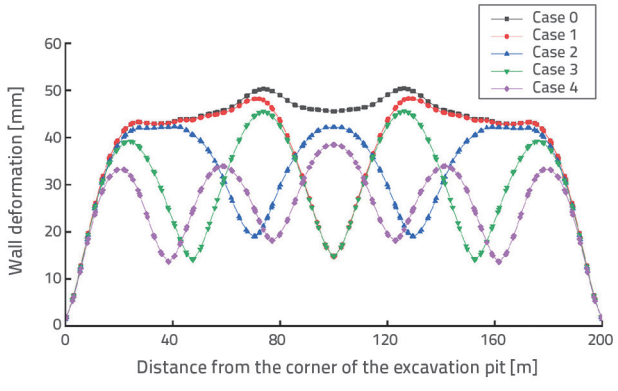

Figure 8. East-wall deformation distribution diagram

A comparative analysis of the deformation data across different cases found that the cross-wall layouts follow a distinct optimization pattern. Starting from Case 2, where the average spacing between cross walls was less than 1.6 times the pit span (65 m), increasing the number of cross walls led to a gradual decline in the reduction amplitude of the maximum retaining wall displacement. Therefore, when cross wall spacing falls below 1.6 times the pit span, the cost-effectiveness ratio of adding cross walls requires special consideration. Notably, in Case 3, despite installing three cross walls, their overlapping with support struts resulted in incomplete utilization of strut stiffness, creating a "shielding effect." To avoid stiffness concentration, it is recommended that the spacing between the cross walls and support struts should be maintained at least 15 m.

3.3. Axial force servo-controlled concrete struts

Six concrete horizontal supports were installed in Zones B and C, with the second to fifth struts utilizing axial-force servo-controlled technology. Conventionally, this technology has been applied to steel struts. However, owing to the limited stiffness of steel components and the high plane and space requirements for the layout, the application of this technology is relatively restricted to large-scale or irregularly shaped excavations.

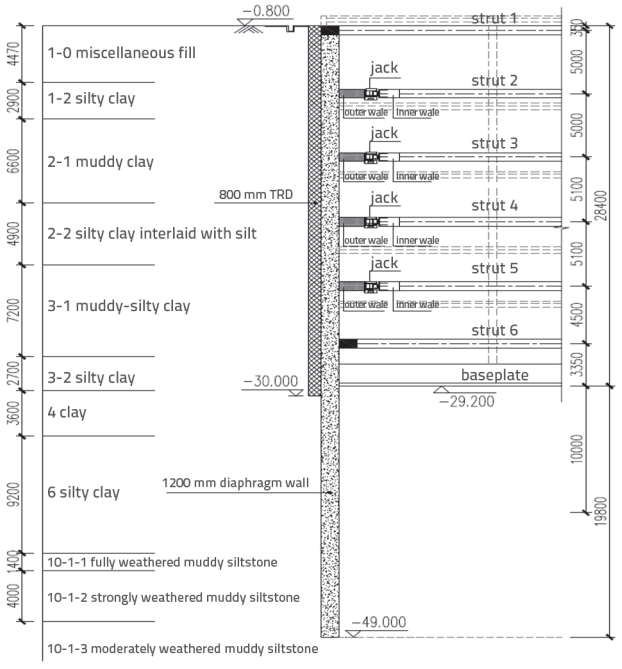

Figure 9. Schematic of axial force servo-controlled strut section

In this project, a double-wale structure was innovatively designed to incorporate axial force servo-controlled technology into a concrete strut system, thus simultaneously leveraging the advantages of the concrete strut's high overall stiffness and strong adaptability. This represents the first large-scale application of servo-controlled axial-force concrete struts in deep excavations of such magnitudes.

The axial force servo-controlled system consists of a main control system, numerical control hydraulic pump station, and

Table 4. Prestress values of the cross braces

Strut	Zone B		Zone C	
	One jack [kN]	**Per meter** [kN/m]	**One jack** [kN]	**Per meter** [kN/m]
Strut 2	1500	750	1800	900
Strut 3	2300	1150	3000	1500
Strut 4	2600	1300	3200	1600
Strut 5	2600	1300	3200	1600

servo-controlled loading devices, which can apply axial force in real time and automatically regulate the system. Servo-controlled loading devices were arranged on the east side, with Zones B and C equipped with 54 and 60 jacks per level, respectively. They were arranged in groups of three and placed between the inner and outer wales; the layout plan is shown in Figure 2. The force transmission path without prestress is as follows: soil and water pressure outside the pit→retaining wall→outer wale→force transmission pier→inner wale→strut. After applying the prestress, the force transmission path becomes: soil and water pressure outside the pit→retaining wall→outer wale→jack→inner wale→strut. To enhance the deformation coordination capability of the strut system, a 200 mm-thick concrete slab was set in the range of the cross braces and the east side truss.

Restraining the deformation of the retaining wall by increasing the prestress of the strut at depth is necessary to ensure the maximum precompression deformation of the concrete struts. In addition, the positive and negative displacements of the retaining wall repeatedly disturb the soil outside the pit, which is not conducive to the long-term protection of environmental objects. Therefore, the application of prestress in this project involved a one-step approach, and the prestress value was taken as 80% of the design value of the axial force of each strut. During implementation, adjustments were made according to the actual deformation; however, the compressive bearing capacity of the strut member cross-section must not be exceeded. As Zones B and C belong to two different contract sections, the specifications of the jacks used were different, with rated loads of 350 and 500 t, respectively. The final prestress values applied to the cross-braces are listed in Table 4. Considering that the overall stiffness of the strut in the corner brace and side truss areas was relatively low, the applied prestress was 50% that of the cross brace.

After the concrete strength of each strut reached C30, loadings of 40%, 60%, 80%, and 100% of the designed value were incrementally applied. Each loading stage was performed only after the travel of the jack had stabilized from the previous stage. The axial force of the struts exhibited the following four stages of change during the excavation:

1. Initial loading period: The concrete struts experience continuous deformation under compression, and the prestress is frequently lost and automatically compensated for, increasing the travel of the jacks.
2. Stress equilibrium period: The axial force on the struts reaches a balance with the external soil and water pressures, and the strut axial force begins to fluctuate within a normal range depending on the temperature changes.
3. Prestress compensation period: During the time from excavation of the next support to loading, prestress loss occurs again, requiring automatic compensation, which results in a corresponding increase in the travel of the jacks.
4. Stress re-equilibrium period: After the axial force on the struts and the external soil and water pressure re-establish equilibrium, the axial force maintains its normal fluctuation with the temperature changes.

Although the current system applies prestress in a one-step approach, future iterations could incorporate real-time dynamic algorithms integrated with automated monitoring and artificial intelligence technology to automatically adjust axial forces based on wall displacement thresholds, a strategy already implemented in tunnel engineering [25].

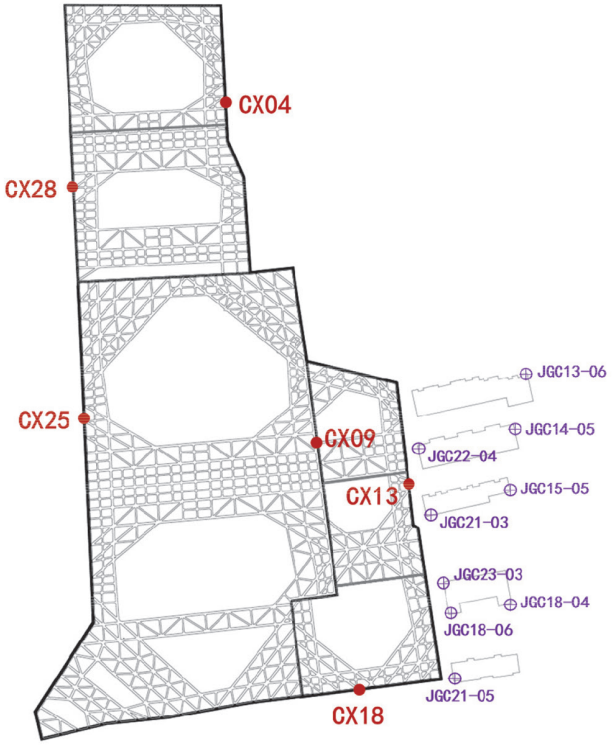

Figure 10. Layout plan for main monitoring points

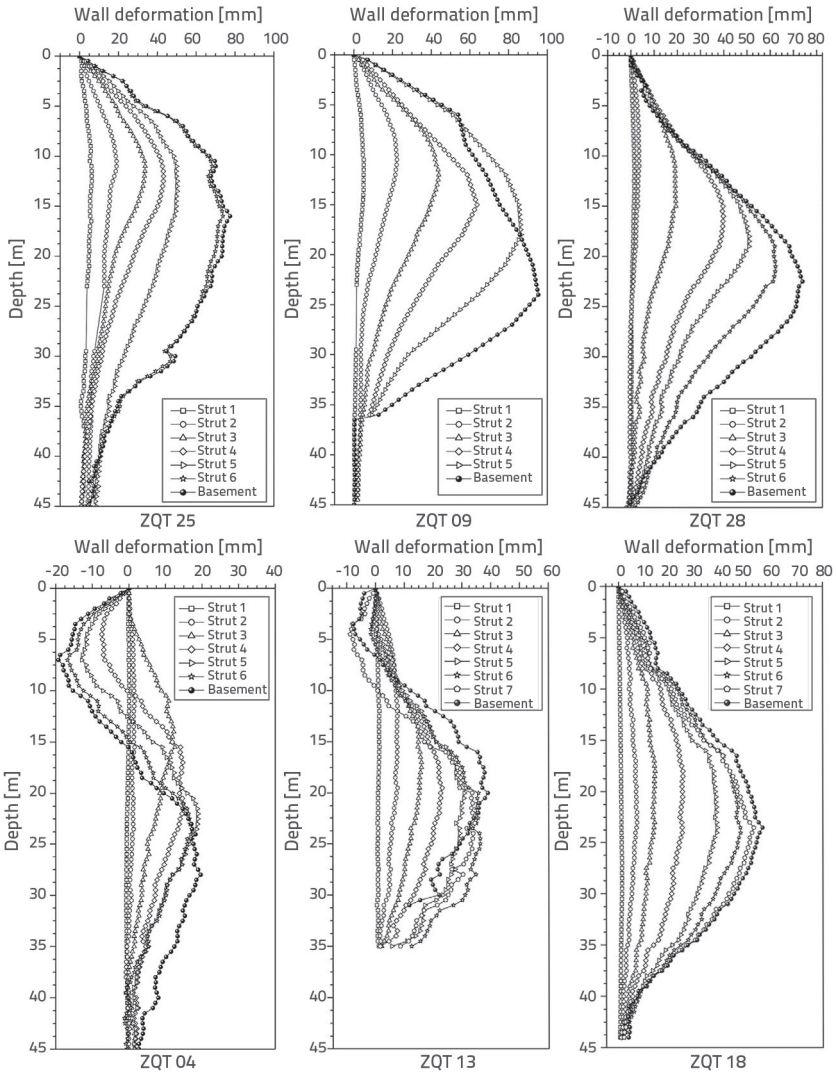

Figure 11. Horizontal displacement curve of the retaining wall

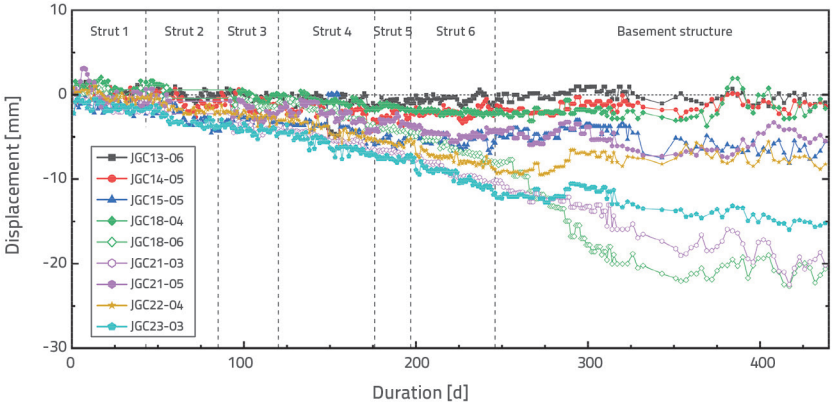

Figure 12. Time history curve of the settlement of shallow-foundation buildings on the east side

4. Field measurement and analysis

The project began with the construction of a pile foundation in July 2019. The pile foundation in Zone A was completed first in November 2020, followed by excavation work; however, work on the remaining pile foundations continued in Zones B and C. By February 2022, the foundation slab in Zone A was completed, and upward construction of the basement structure began concurrently with the excavation of Zones B and C. The entire underground structure was finalized in May 2023. Consequently, there were overlapping construction activities in Zones A, B, and C, including pile construction, earthwork excavation, and strut removal.

The maximum horizontal displacement of the retaining wall in Zone A was 100.60 mm, which was located at the midsection on the eastern side of monitoring point CX09. Correspondingly, the maximum horizontal displacement at the midsection on the west side of monitoring point CX25 was 77.47 mm. The difference in deformation between the two is related to the unfavorable construction conditions during the excavation period in Zone A, where pile foundation construction was simultaneously conducted in Zone C on the east side, and there was a larger overload outside the pit. In addition, according to the displacement curves for the last two conditions at monitoring point CX09, the deformation above the bottom of the pit rebounded. This indicates that during the construction of the basement structure in Zone A, while earthwork excavation and strut installation were underway in Zone C, the partition wall experienced a small-amplitude oscillation owing to the difference in conditions on both sides.

A comparison of the horizontal displacement curves of the two groups of retaining walls in Zones B and C revealed that the deformation curves of the walls without axial-force servo-controlled devices had a typical distended belly shape. In contrast, the deformation curve of the east wall with axial force servo-controlled devices was "S"-shaped, with the upper part of the wall exhibiting negative displacement, and the position of the maximum displacement depth was significantly lowered. The S-shaped curve indicates that the axial force servo-controlled concrete strut technology can effectively control the deformation of the retaining walls. When the applied prestress is excessively large, it can push the retaining walls outward, resulting in negative displacement.

Therefore, the servo-controlled prestress should be set cautiously, preferably in combination with real-time dynamic adjustment based on monitoring, to avoid dual-direction deformation of the retaining walls both inward and outward from the pit, which could cause double superimposed disturbances to the environment.

Figure 12 illustrates the development of the settlement deformation of shallow-foundation buildings on the east side during the entire construction period. As the excavation progressed, the buildings gradually underwent deformation, particularly after the excavation of the third strut, and the rate of settlement began to increase, which may have been related to the excavation reaching the muddy clay stratum. After the foundation slab was poured, the settlement gradually stabilized. By the completion of the basement structure, the maximum settlement of the buildings was mostly controlled to within 20 mm with minimal differential settlement, achieving the control target of ensuring the safety and normal use of residential buildings.

5. Conclusion

With the expanding development of urban underground space resources, excavation engineering will inevitably evolve into larger, deeper, and more complex work. For the deformation control of deep and large excavations in complex environments in soft soil areas, simply increasing the rigidity of the support structure not only fails to achieve the desired deformation control effects but also wastes resources. This paper, which considered the five-story deep excavation of the Hangzhou Hang Lung Plaza, introduced the application of technologies such as zoned excavation, cross walls, and axial force servo-controlled concrete struts. The field measurement data indicated that the comprehensive use of the aforementioned active protection technologies achieved excellent results in controlling the deformation in the retaining walls and adjacent shallow-foundation building clusters, thus ensuring the smooth implementation of the entire project.

Zoned excavation measures are commonly used in deep and large excavations where theoretical research and practical experience are extensive. Cross walls are a proven deformation control method, and their planar layout must balance the stiffness compatibility and economic feasibility. In the absence of prior experience, the spacing between the cross walls can be designed as 1.6 times the excavation span. Future research should prioritize parameter sensitivity analysis, studies on combined reinforcement techniques, and the development of spatiotemporal effect prediction models to advance the standardized application of cross-wall technology. To formulate a reasonable loading design, axial-force servo-controlled concrete struts require further analysis in terms of the number of servo-controlled struts and the impact of loading on the upper and lower struts. This project is the first large-scale application of axial force servo-controlled concrete strut technology to deep excavation work in Zhejiang Province. The double-wale design solved the problem of force transmission between the retaining wall and strut system, achieving the integration of the axial force servo-controlled concept with traditional concrete struts and providing an effective deformation control strategy for deep and large excavations in soft soil areas.

REFERENCES

[1] Jing, Y., Li, L., Li, J., Chen, H.: Performances of a large-scale deep excavation with multi-support types and zoned excavation technique in Shanghai soft soil. Canadian Geotechnical Journal, 62 (2025), pp. 1-20.

[2] Chiu, H.W., Hsu, C.F., Tsai, F.H., Chen, S.L.: Influence of different construction methods on lateral displacement of diaphragm walls in large-scale unsupported deep excavation. Buildings, 14 (2024) 14, Paper No. 23.

[3] Tang, Y., Zhao, W., Zhou, J.: The deformation of retaining piles and ground surface under various support systems during deep excavation. Geoenvironmental Disasters, 4 (2017), Paper No. 22.

[4] Maher, T., El-Nimr, A., Basha, M., Abo-Raya, M.M., Zakaria, M.H.: General deformation behavior of deep excavation support systems: A review. Global Journal of Engineering and Technology Advances, 10 (2022) 1, pp. 039–057.

[5] Gong, X.N.: Deep excavation engineering design and construction manual. Beijing: China Architecture & Building Press, 1998.

[6] Liu, X.W., Li ,B.H., Chen, W.L.; Control technology of influence on adjacent metro tunnels by deep and large excavation of 6 Basements in Thick Soft Soil. Building Structure, 52 (2022) 15, Paper No. 137.

[7] Xu, C., Chen, Q., Wang, J., Hu, W., Fang, T.: Dynamic deformation control of retaining structures of a deep excavation. Journal of Performance of Constructed Facilities, 30 (2016) 4, Paper No. 04015071.

[8] Gordon, T.C. Kung, C., Juang, H., Hsiao, E.C.L., Hashash, Y.M.A.: Simplified model of wall deflection and ground surface settlement caused by braced excavation in clays. Journal of Geotechnical and Geoenvironmental Engineering, 133 (2007) 6, pp. 731-747.

[9] Yang, X.L., Cao, G.Q., Zhou, P.H.: Design of retaining structure for five-story basement deep excavation of Hangzhou Guoda City Plaza. Building Structure, 42 (2012) 8, Paper No. 94.

[10] Yin, Y.H.: Design and practice of deep and large excavations adjacent to metro in thick soft soil strata Chinese Journal of Geotechnical Engineering, 41 (2019) Suppl.1, Paper No. 129.

[11] Hou, S.N., Yue, J.Y., Zhou, Y.: Design and practice of deep and large excavation for a sports building in a complex environment. Journal of Building Science and Engineering, 38 (2021) 6, Paper No. 119.

[12] Ou, C.Y., Hsieh, P.G., Lin, Y.L.: Performance of excavations with cross walls. Journal of Geotechnical and Geoenvironmental Engineering, 137 (2011) 1, Paper No. 94.

[13] Hsieh, P.G., Ou, C.Y., Lin, Y.L.: Three-dimensional numerical analysis of deep excavations with cross walls. Acta Geotechnica, 8 (2013), pp. 33-48.

[14] Ou, C.Y., Hsieh, P.G., Lin, Y.L.: Performance of excavations with cross walls. Journal of Geotechnical and Geoenvironmental Engineering, 137 (2011) 1, pp. 94-104.

[15] Zeng, C.F., Wang, S., Song, W.W., et al.: Control effect of inner partition wall on deformation of soft soil area metro deep excavation induced by groundwater extraction before excavation. Chinese Journal of Rock Mechanics and Engineering, 40 (2021) 6, Paper No. 1277.

[16] Nangulama, H., Zhou, J.: Deformation control monitoring of basement excavation at field construction site: A case of hydraulic servo-controlled steel enhancement geotechnology. Advances in Civil Engineering, 2022, Paper No. 6234581.

[17] Lapčević, R., Vojnović, B., Lokin, P., Bogdanović, S.: Realization and protection of deep flysch excavations in complex geotechnical conditions. Gradevinar, 1 (2015), pp. 33-42.

[18] Chen, B., Yan, T., Song, D., Luo, R., Zhang, G.: Experimental investigations on a deep excavation support system with adjustable strut length. Tunnelling and Underground Space Technology incorporating Trenchless Technology Research, 115 (2021), Paper No. 104046.

[19] Li, M.G., Demeijer, O., Chen, J.J.: Effectiveness of servo-controlled struts in controlling excavation-induced wall deflection and ground settlement. Acta Geotechnica, 20 (2020).

[20] Zhao, S.M., Cui, Y.G., Chen, W.D.: Finite element analysis of deep excavation considering creep of concrete support. Building Science, 25 (2009) 11, Paper No. 46.

[21] Wei, J.H., Lu, C.L., Luo, C.H.: Design and practice of prestressed concrete servo-controlled support in deep excavation of soft soil. Geotechnical Engineering Technology, 37 (2023) 6, Paper No. 737.

[22] Zou, W.J.: Analysis of the influence of prestressed reinforced concrete supports on the deformation of adjacent metro tunnels by deep excavation in soft soil areas. Foundation Treatment, 5 (2023) 2, Paper No. 152.

[23] Tabaroei, A., Sarfarazi, V., Pouraminian, M., Mohammadzadeh, D.S.: Evaluation of behavior of a deep excavation by three-dimensional numerical modeling. Periodica Polytechnica Civil Engineering, 66 (2022) 3, pp. 967-977.

[24] Hsu, C.F., Kuan, C.F., Chen, S.L.: Three-dimensional numerical analysis on the influence of buttress wall removal timing on the lateral deformation of diaphragm walls during deep excavation. Buildings, 13 (2023), Paper No. 2678.

[25] Shen, J.: Analysis and countermeasures of mutual influence of ultra-large scale excavation group excavation. Chinese Journal of Geotechnical Engineering, 34 (2012, Suppl.1, Paper No. 272.

[26] Lv, J., Zheng, B., Liu, Z., Huang, J.: Controlled shaped-charge blasting technology for deep underground tunnel engineering, GRAĐEVINAR, 75 (2023) 10, pp. 997-1011, https://doi.org/10.14256/JCE.3768.2023